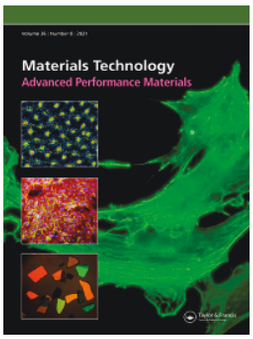

Materials Technology
Advanced Performance Materials

ISSN: (Print) (Online) Journal homepage: https://www.tandfonline.com/loi/ymte20

Mechanistic understanding of the interaction of cells with nanostructured surfaces within the framework of biological functions

R.D.K. Misra & Aladin M. Boriek

To cite this article: R.D.K. Misra & Aladin M. Boriek (2023) Mechanistic understanding of the interaction of cells with nanostructured surfaces within the framework of biological functions, Materials Technology, 38:1, 2216529, DOI: 10.1080/10667857.2023.2216529

To link to this article: https://doi.org/10.1080/10667857.2023.2216529

Published online: 23 May 2023.

MATERIALS TECHNOLOGY
2023, VOL. 38, NO. 1, 2216529
https://doi.org/10.1080/10667857.2023.2216529

Mechanistic understanding of the interaction of cells with nanostructured surfaces within the framework of biological functions

R.D.K. Misra[a] and Aladin M. Boriek[b]

[a]Department of Metallurgical, Materials, and Biomedical Engineering University of Texas at El Paso, El Paso, TX, USA; [b]Departments of Medicine and Molecular Physiology and Biophysics, Baylor College of Medicine One Baylor Plaza, Houston, TX, USA

ABSTRACT

The interaction of nanostructured surfaces with cells is complex and has a profound impact on the behaviour of cells by influencing their adhesion, migration, proliferation, and differentiation. Our studies highlighted the contrasting effects of nanostructured and microstructured surfaces on biological functions. Such contrasting effects include the relative influence of physical and chemical attributes of the nanoscale surface compared to the microscale counterpart. These attributes lead to an altered cellular activity at the bio-nano interface through modulating cell adhesion, proliferation of cells and synthesis of functional proteins. Physical and chemical changes induced by the nanostructure are likely to promote cell adhesion, without introducing chemical functionalities on the surface. This represents a significant advance beyond guiding the tailoring of cellular functionality at the bio-nano surface. This would yield an improved understanding of a rational design of biotic/abiotic interfaces that can promote optimal biological responses, leading to the development of new biomedical technologies.

ARTICLE HISTORY
Received 3 May 2023
Accepted 17 May 2023

KEYWORDS
Biomedical stainless steel; nano-grained; grain boundary parameter; cellular functions

Developing nanoscale structure for studying nano-bio-interactions on bulk metallic materials

Stainless steels and titanium are two widely used alloys that are utilized in biomedical devices for knee and hip joints [1–3]. However, these permanently attached artificial metallic devices break down more frequently even in the physiological environment. Failure of such devices occurs because of insufficient bone build-up around the implants, making them loose and triggering less interaction of cells with the surrounding implant surface. Other reasons for such failure include the generation of metallic debris due to wear absorption near the implant. This would lead to attacking the body's immune system, leading to inflammation, necrosis and loss of bone surrounding the implant [1–3]. In this regard, nano-structuring of implant materials is a promising approach for the next generation of biomaterials [2]. As demonstrated in sections 2 and 3, the nanoscale surface favourably modulates cell–implant interactions in the biological environment, promoting bone growth. Simultaneously, the high strength of the nano-grained (NG) metal implant provides wear resistance to withstand long-term loading and is in addition to a thinner and reduced mass leading to a high strength/weight ratio.

In recent years, surface modification methods including heat treatment [2–4], powder metallurgy [5] and sintering [6,7] have been explored to obtain ultrafine structures on the surface of metals and alloys to promote modulation of cellular activity [6–11]. Approaches have been explored to obtain bulk NG and ultrafine-grained (UFG) metals and alloys from the viewpoint of long-term stability of implants and increase in biological functions [12,13]. Those include thermo-mechanical processing and laboratory-scale severe plastic deformation approaches such as equal channel angular pressing (ECAP) [13–16], accumulative roll bonding (ARB) [17–19], high-pressure torsion (HPT) [20–23], multiple compression [24] and upsetting extrusion [25]). It is important to recognize that the ductility of NG materials produced by severe plastic deformation methods is significantly low compared to CG materials. A high strength, high ductility combination is an important mechanical property requirement for a longer life of metallic formable implants [26–29]. Misra's group recently addressed the issue of high strength-high ductility combination in biomedical stainless steel by developing the concept of phase reversion-induced NG materials [30–32]. In this approach, severe cold deformation (~60–80% reduction in thickness) of the austenite phase of Fe at room temperature has led to the strain-induced transformation of face-centred cubic (FCC) austenite

CONTACT R.D.K. Misra dmisra2@utep.edu Department of Metallurgical, Materials, and Biomedical Engineering University of Texas at El Paso, 500 West University Avenue, El Paso, TX 79968, USA

to body-centred cubic (BCC) martensite phase. Upon annealing at 700–800°C for short durations of 10-100 s, the martensite phase transforms back to austenite via either a diffusional-reversion or shear mechanism [30–32]. The grain size in the phase reversion concept is controlled by temperature-time annealing treatment of the severely cold deformed material, where a lower temperature and time that completely reverts strain-induced martensite to austenite provides finer grain size. Pre-dominance of dislocation-cell type structure in the severely deformed martensite phase is an important criterion for obtaining NG structure. Such an approach would enable NG structure without compromising ductility. Figure 1 shows that with the decrease in grain size from the coarse-grained (CG) to the NG regime, there is a significant increase in strength without compromising ductility. This would indicate an increase in the strength of the NG structured material with no change in its ability to absorb energy before fracture. It is important to recognize that the resistance to wear would benefit from high strength. On the other hand, the production of medical devices would require the maintenance of ductility [33].

The high ductility of conventional CG stainless steel is associated with a gradual transformation of austenite to martensite, and this leads to an increase in the rate of strain hardening and postpones the initiation of localized necking. However, the strain accommodation mechanism shifted from transformation-induced plasticity (TRIP) to twin-induced plasticity (TWIP) as the structure transitioned from CG to NG [30.32]. The exceptional ductility of the 'high strength' NG structure resulted from nanoscale twinning, which played a vital role as a deformation mechanism. Conversely, in the 'low strength' CG structure, the ductility was also high, but it was primarily due to the formation of strain-induced martensite. By utilizing phase-reversion, it is possible to achieve varying grain sizes within a single material while maintaining the same processing parameters [30–32].

Our objective is to provide an overview and perspective of cellular activity in terms of cell adhesion, proliferation and synthesis of proteins, mineralization and differentiation of cells on the nano-grained surface (NG – grain/crystal size in the nanometre range) in comparison with the coarse-grained (CG – grain size in the micrometre regime) counterpart. Second, we will identify the chemical and physical attributes that could potentially contribute to the mechanism responsible for the significant difference in the cellular activity on the NG surface compared to the CG counterpart. This would provide a strong rationale for follow-up mechanistic studies that will be reported later.

Experimental approach to bio-nano interactions

The different grain sizes (Figure 1) studied were obtained by the phase reversion concept [30–32], briefly described in section 1. NG (NG with few ultrafine grains) and CG structure were obtained by changing the percentage of cold deformation and annealing temperature-time sequence. The grain size of fine-grained (FG) structure to NG regime was determined from at least 25 transmission electron microscopy (TEM) micrographs using the ASTM linear-intercept method, while the grain size of CG steel was measured using light micrographs. The average grain size of CG steel was 22 ± 3 μm (Figure 1a) with a yield strength of 350 ± 5 MPa and mechanical strain of nearly ~40%. The NG steel with an average grain size of 90 ± 8 nm provided an excellent combination of yield strength of 800 ± 7 MPa and mechanical strain of nearly 38%. This combination of NG structure and its mechanical properties is obtained in bulk NG materials [30–32].

We briefly describe below the experimental methods that were used to study cell–substrate interactions within a biological setting. The experimental protocols are described in some detail elsewhere [34–38].

Selection of cells

Osteoblasts are responsible for the formation of new bone. They first differentiate from the precursor

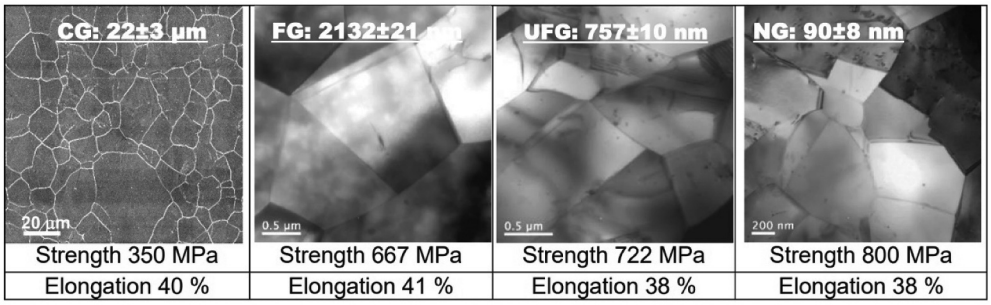

Figure 1. Light micrograph of CG stainless steel with an average grain size of 22 ± 3 μm and TEM micrographs from NG to FG. NG: nano-grained; UFG: ultrafine-grained; FG: fine-grained; CG: coarse-grained [30–33]. NG had a few ultrafine grains (UFG), hence referred to as UFG/NG in Figures 2-6.

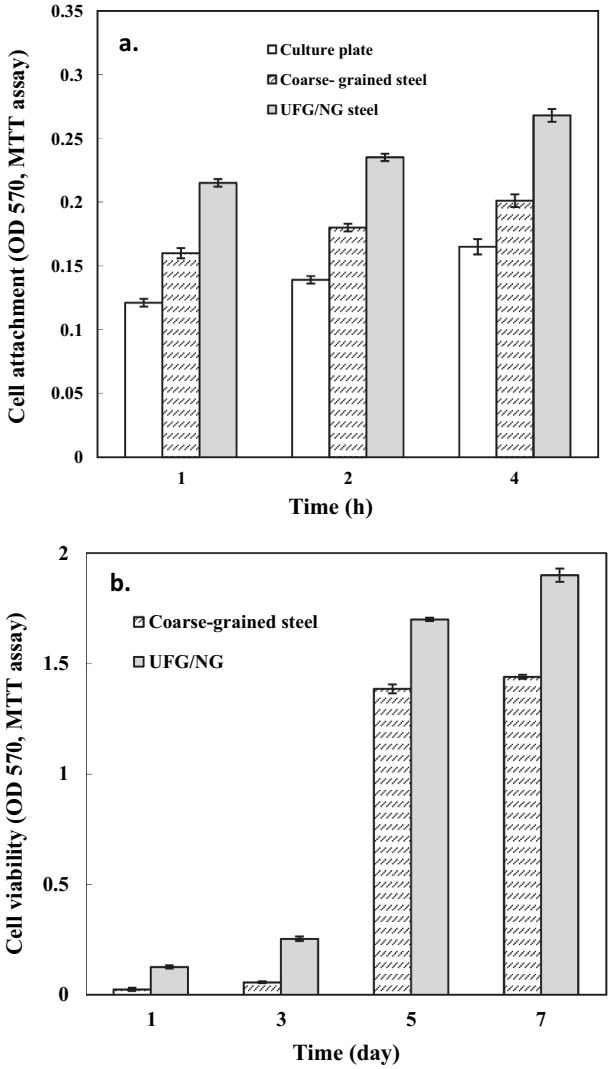

Figure 2. Histograms represent (a) initial cell attachment after culture time of 1–4 h and (b) metabolism of pre-osteoblasts after 1–7 days on NG/UFG and CG substrates using MTT assay. The pre-osteoblasts showed significantly better cell attachment to NG/UFG substrate than CG material and control polystyrene culture plate. The higher attachment on NG/UFG substrates in comparison to CG substrate was visible within the first hour of culture [34–38].

adjacent to the bone surface. Thus, they were selected to study the cellular activity on the surface of austenitic stainless steel [29–32].

Sample preparation to similar nanometric smoothness

Surface roughness is an important parameter that influences cellular response. Thus, all the samples were mechanically polished to almost similar surface nanometric roughness using a Buehler Vibromet vibratory polisher with a suspension of 20 nm colloidal silica in water for 12 h.

Our objective was to examine the impact of nanoscale structure (NG versus CG) while minimizing the influence of large-scale topographical features so that the cell–substrate interactions remain unobstructed. The average arithmetic mean roughness, Ra, measured from 3 μm × 3 μm scan area for CG and NG stainless steel was 1.45 ± 0.21 and 1.52 ± 0.29 nm, respectively [34–38].

Cell culture

Cell culture studies were performed using mouse pre-osteoblasts cell line MC3T3-E1 subclone 4 (ATCC, USA). Alpha minimum essential medium (a-MEM, Invitrogen Corporation, USA) supplemented with 10% foetal bovine serum (FBS), penicillin (100 U mL^{-1}) and streptomycin (100 μg mL^{-1}) were used to culture pre-osteoblasts. Polished stainless-steel samples (1 cm^2) cleaned in an ultrasonic bath with ethanol, followed by deionized water, were wrapped individually in gauze and sterilized in an autoclave. Identical volumes of pre-osteoblasts with 80–85% confluence obtained from T-flask cultures were used to seed onto the disk samples [34–38].

Briefly, cells were washed with phosphate-buffered saline (PBS), incubated with 0.25% trypsin/0.53 mM EDTA for 5–7 min to detach the cells from the Petri dish, dispersed cells in trypsin/EDTA, transferred to a centrifuge tube and centrifuged at 2000 rpm for 5 min. Cell pellets obtained after centrifugation were re-suspended in a culture medium and dilution was carried out using a culture medium to obtain the required cell concentration. Subsequently, the sterilized steel disks were placed in a 24-well plate and incubated with cell suspension at 37°C in a humidified atmosphere with 5% CO_2 and 95% air. Polystyrene 24-well culture plates were used for control experiments [34–38].

Cell attachment

The 'initial attachment' of cells on NG and CG substrates was evaluated as follows: Fluorescent labelling of nucleic acids was performed to assess the number density of osteoblasts on substrates using a fluorescence microscope (Nikon E600). Pre-osteoblasts (10,000 cells/cm^2) were seeded on the surface of substrates and incubated for 1, 2 and 3 h, at 37°C in a CO_2 incubator (5% CO_2 and 95% air). After the end of the prescribed period, the cells were stained with the nucleic acid dye, Hoechst 33,342. Next, cell-seeded disks were washed twice with PBS and incubated (10 μg dye/ml PBS) for 10 min at 25°C before viewing under a fluorescence microscope with excitation and emission of 346/442 nm, respectively. Cell nuclei appeared as blue-fluorescent spots. The number of cells in each of the five random fields/substrate was counted using the image analysis software and the average count/substrate was expressed as cells/cm^2 of the substrate area [34–38].

Cell proliferation, morphology and morphometry of osteoblasts

Scanning electron microscopy (SEM) was used to observe the spreading pattern, morphology and morphometry of pre-osteoblasts. Cell-seeded samples were grown for 1, 2, 3, 6 and 20 days, and then fixed with 2.5% glutaraldehyde in 0.1 M cacodylate buffer pH 7.4 for 20 h; rinsed with PBS; dehydrated with a graded series of ethanol (25–100%) and dried in a critical point dryer. The samples were sputter-coated with gold and examined under a JEOL 6300F field emission SEM. The difference in spread and morphology provided details on the time course of growth and the extent of biomineralization. The mineralization was studied using EDS analysis in SEM. Simultaneously, ImageJ analysis software was used to quantify Feret's diameter of cells, area and perimeter. This analysis was important in identifying differences in cell–surface interactions between NG and CG structures [34–38].

Bio-nano interactions: cellular activity

Nanograined (NG) versus coarse-grained (CG) structure

The attachment of cells (Figure 2 and blue spots in Figure 3) on both the steel substrates indicated good cytocompatibility with the pre-osteoblasts. However, the cells had greater attachments to the NG substrate compared to the CG substrate. The greater attachment was visible within 1 h of cell culture. This suggested that the cell attachment to the surface was influenced by grain size and was not a function of cell development or adaptation over time. Thus, the NG structure had a strong cell adhesion ability compared to the CG structure. Cell adhesion to the surface is critically important for subsequent cellular activities including proliferation and differentiation [34–38].

Proliferation and morphology of attached cells and cytoskeletal development

The cell spreading pattern (Figure 4) exhibited a different morphology on NG and CG surfaces. On the CG surface, the cell morphology after 24 h culture was compact with a less well-defined periphery, while the NG surface induced a significant change in cell morphology, such that the cells were elongated and were spread uniformly with less well-defined boundaries (see Figure 4). On the other hand, the cells on the NG surface exhibited a flattened morphology with star-like shapes and several cytoplasmic extensions that appear to overlap and form cytoplasmic bridges. This indicates a substantial level of cell–substrate interactions (see Figure 4). Thus, the extent

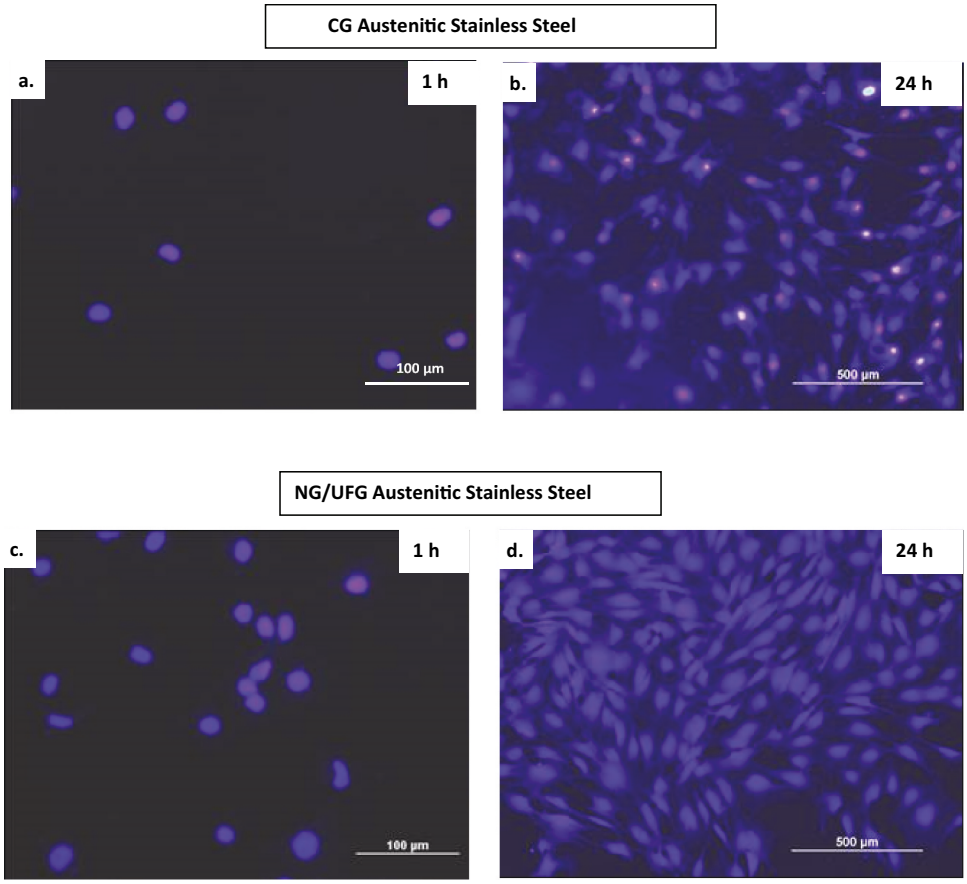

Figure 3. Fluorescence microscopy of pre-osteoblasts nuclei stained with Hoechst 33,258 (1 µg/ml). Cell nuclei showed blue fluorescence after staining. After 1 h and 24 h culture on CG (a, b) and NG/UFG austenitic stainless steels (c, d). Cell density on the surface of NG/UFG austenitic stainless steel was higher than on CG austenitic stainless steel [34–38].

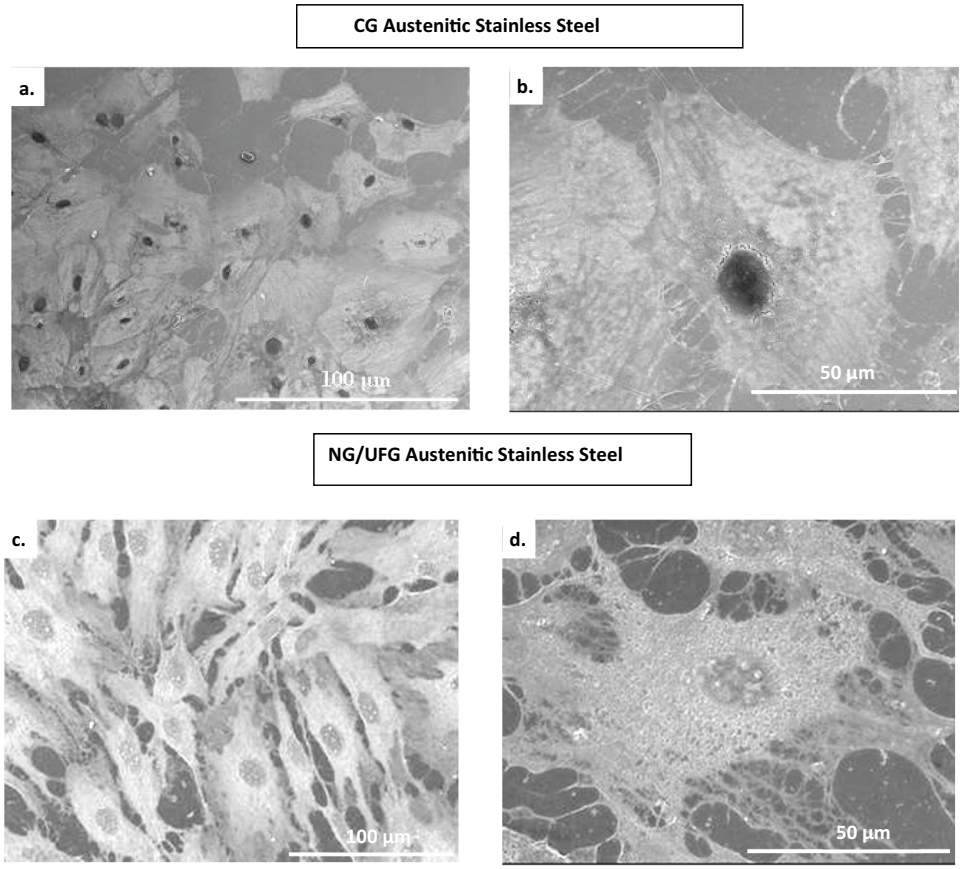

Figure 4. Scanning electron micrographs of pre-osteoblast cultured for 24 h on CG austenitic stainless steel (a, b) and on NG/UFG austenitic stainless steel (c, d). At low magnification, improved cell proliferation with abundant extracellular matrix formation on the NG/UFG surface. High magnification (b, d) shows a higher extent of spreading and interconnectivity on the NG/UFG surface than on CG austenitic stainless steel. On CG austenitic stainless steel, the cell morphology is circular with higher longitudinal cytoskeletal alignment than on NG/UFG austenitic stainless steel cells, which show numerous cellular extensions indicative of extensive attachment to and interaction with the substrate [34–38].

of cell spreading was remarkably greater on the NG surface compared to the CG surface. Additionally, the 3D network of extracellular matrix macromolecules that offer structural and biochemical support to neighbouring cells and mineralization was found to be more pronounced on the NG substrate as compared to the CG substrate. This is suggestive of enhanced biological interactions between the cells and the nano surface.

Organization of key proteins

Two prominent proteins that affect cell–substrate interactions are actin and vinculin. Immunofluorescence microscopy using antibodies was used to study the key proteins because the approach enables us to study in detail the organization of key proteins, sub-cellular features including cytoskeleton, focal adhesion contacts and cell differentiation besides cell adhesion and proliferation. Pre-osteoblasts were seeded on NG to CG surface and cultured for 2 days and stained using standard protocol [34–38].

Using both the NG and CG surfaces we examined the cytoskeletal proteins, actin and vinculin, which are linked to cellular activity. The expression of vinculin and actin that form focal contacts and stress fibres showed higher expression levels at the edges and well-defined stress fibres on NG steel compared to that on CG steel (Figure 5). This was confirmed by quantitative analysis of proteins (Figure 7), in terms of pixel-based density of the recorded fluorescence micrographs using an image analysis software. The pixel density was calculated in two different ways, cell-based expression (total pixels/cell number) and cell area-based expression (total pixels/total cell area). Similarly, fibronectin expression was greater on the NG surface than that on the CG surface, as apparent from the distinct network with a stronger intensity of fluorescence of immunostained fibronectin (Figure 6) [34–38].

Quantitative analysis

Furthermore, a quantitative analysis of cytoskeletal development, cytomorphometry (cell area, perimeter, and Feret's diameter), using a combination of fluorescence micrographs and image analysis tools also indicated significant differences between cellular response on CG and NG substrates (Figure 5), corroborating the qualitative observations of Figures 4 and 5. The data obtained were normalized to control experiments and expressed as a mean of at least three replicates ± SD

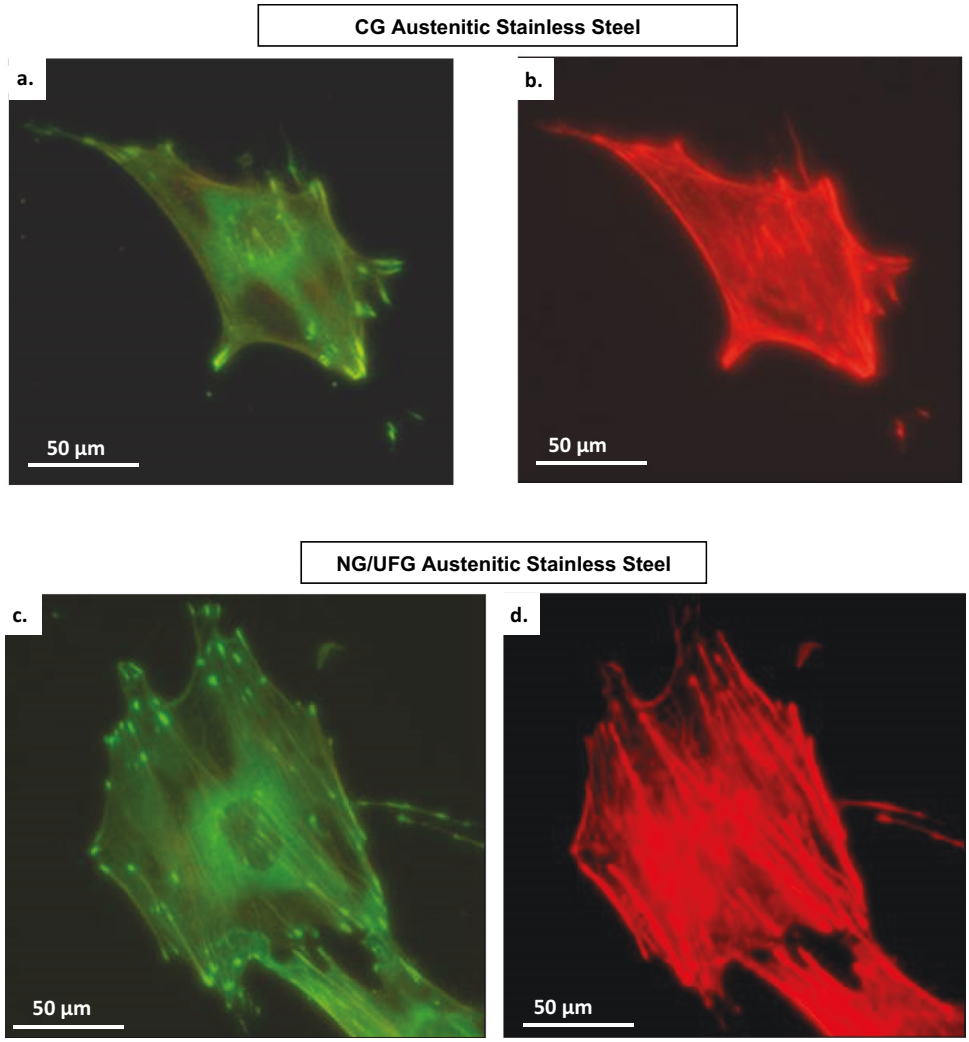

Figure 5. Organization and assessment of focal contacts and actin stress fibres of pre-osteoblasts after 2 days culture on CG (a,b) and NG/UFG (c,d) stainless steel substrates. Vinculin (a, c) staining shows a larger number of focal contact sites in pre-osteoblasts grown on the surface of NGUFG (c) compared to cells grown on the CG surface (a). The higher number of focal adhesion points corresponded well with a higher number of actin stress fibres on NG/UFG steel than on CG steel (b) [34–38].

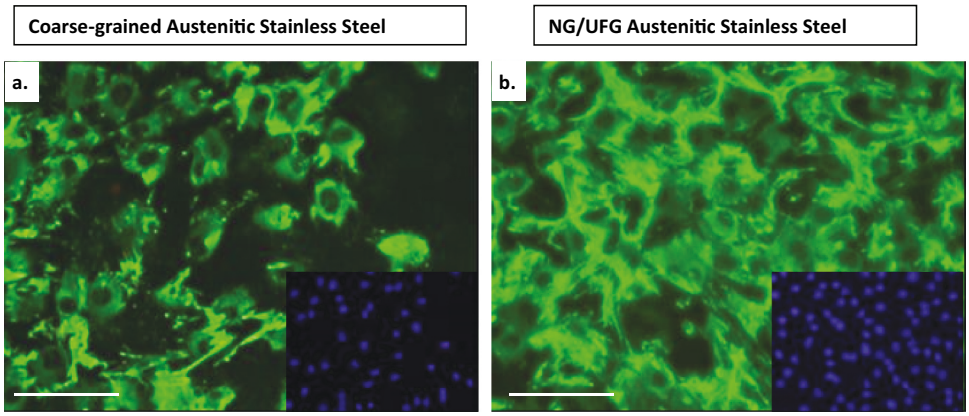

Figure 6. Fluorescence micrographs representing immunocytochemistry of fibronectin expressed by pre-osteoblasts after incubation for 2 days on (a) CG and (b) NG/UFG stainless steel surface. A higher fluorescence intensity and an expanded network of fibronectin expression along with a higher cell density is observed after labelling of cell nuclei with 4′,6-diamidino-2-phenylindole (DAPI) (inset micrographs) [34–38].

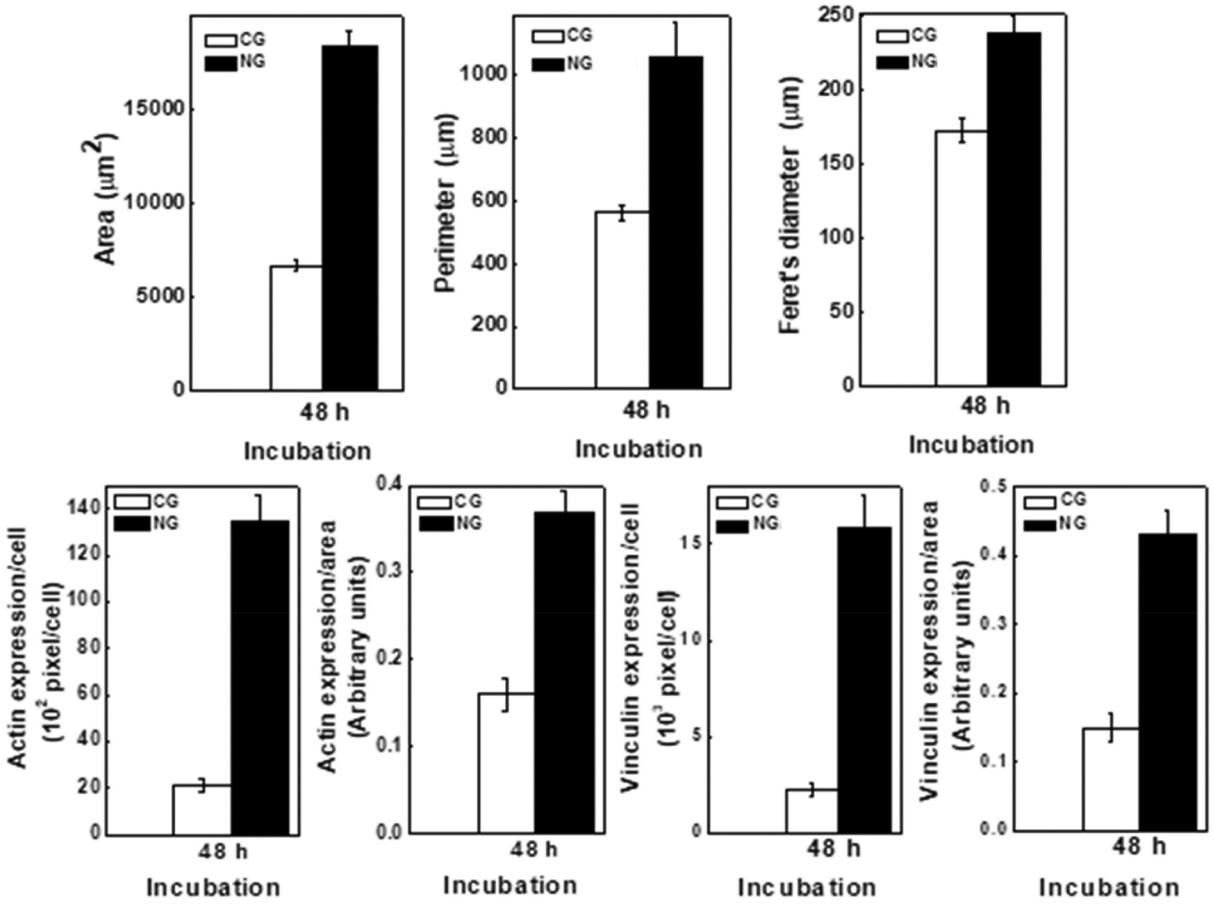

Figure 7. Cytomorphometric evaluation of cell parameters (cell area, perimeter, Feret's diameter) using micrographs of the type presented in Figure 3 and expression level of proteins (actin and vinculin) (Figure 5) by densitometry approach using the image analysis software. Data are represented as mean ±SD ($n = 5$) $p < 0.05$. CG and NG show a statistical difference [34–38]..

(standard deviation) and statistically analysed. Statistical analysis was performed using a one-way analysis of variance (ANOVA) with a 95% confidence interval [34–38].

Relationship between grain boundary parameters and the bio-physical parameter and average grain boundary length/cell for NG and CG surfaces

Quantification of cells attached to the surface was carried out in detail and was correlated to grain boundary parameters. Analysis of at least 10 light (for CG) and transmission electron (for NG) micrographs indicated significant differences in the average grain boundary length/surface areas and were ~15.5 micrometer/micrometer^2 and ~0.14 micrometer/micrometer^2 for NG and CG structures, respectively. Also, the average distance between grain boundaries and the dimensions of cells was significantly different between the NG and CG structures. Considering a representative average width of osteoblasts of 5–20 micrometer, as seen in Figures 2 and 3, on the NG surface, an attached cell covered ~25–75 grains by width and ~720 grains by length. In striking contrast, a similar average size of a cell on the CG surface covered ~1–3 grains by width and ~15–24 grains by length.

Thus, the NG surface had a significantly greater number of grain boundaries than surface-attached cells. This was based on a computation of a 'biophysical parameter', average grain boundary length per surface-attached cell [39]. Such biophysical parameter considers the physical aspect of the surface, namely, the average grain boundary length/area with the cell characteristic, i.e. the average area of the surface covered by the cells. Table 1 presents interesting data and a positive relationship of cell attachment with biophysical parameters such as the ratio of grain boundary length to surface attached cells. This is supported by our data that showed more than 20 times the average length of grain boundaries/cells were occupied by the cells on the NG surface compared to the CG [33]. The intercept length of ~40–60 nm of the NG surface is similar to the average separation distance of cell adhesion contact or endothelial cells (~40 nm) [33,40].

Interaction process of cells with the NG surface with a high density of grain boundaries

The data in Figures 3–7 demonstrate the potential for the higher density of grain boundaries in the NG structure compared to that of the CG structure to provide greater avenues for cell–surface interactions.

Table 1. Relationship between grain boundary parameters bio-physical parameters and average grain boundary length/cell for NG and CG surfaces [33].

	Average area of the surface covered by the cells (μm^2)	Average total grain boundary length/surface area ($\mu m/micrometer^2$)	Average grain boundary length/cell (μm)
NG	1252.5	15.5	19414
CG	517.8	0.14	71

This would trigger an altered mechano-transduction pathway, potentially leading to a highly mineralized extracellular matrix by the differentiating cells.

Our data show that cell attachment, cell proliferation, cell morphology, the expression level of key proteins, and the degree of mineralization of the extracellular matrix were greater on the NG surface compared to the CG surface. This was established based on comprehensive studies including MTT assay, trypan blue assays, SDS-Page analysis, alizarin red mineralization assay, cytomorphometric analysis of cell parameters, immunofluorescence microscopy, and electron microscopy studies [34–38].

Our studies show that the high density of grain boundaries in the NG structure compared to the CG structure increased the interaction between the cells and its substrate surface. Such interactions would impact cell signalling and mechano-transduction pathways, and this would lead to a highly mineralized extracellular matrix by the differentiating cells. The data suggest that the cells 'globally' interact with the NG surface in a manner like CG. Upon attachment to the surface, the cell explores the surrounding biological environment and migrates via lamellipodia and filopodia, such that their ends establish focal adhesion. This potentially occurs for subsequent migration and communication between cells leading to proliferation and mineralization of the extracellular matrix (ECM) by the differentiating osteoblasts. The filopodial interaction amongst cells is the governing factor in the secretion of ECM, with a consequent influence on maturation and mineralization.

Nanoscale effect and future outlook

Our results demonstrate that the presence of nanoscale features on the surface of NG has a significant effect on how the cells in the biological environment interact with it. This commences with the greater attachment of cells to the nanoscale surface, followed by proliferation, synthesis of proteins, differentiation and mineralization. The CG and NG substrates had identical microstructural constituent (austenite-phase), and near-identical average arithmetic mean roughness, Ra (CG: 1.45 ± 0.21 nm; NG: 1.52 ± 0.29 nm), as determined by an atomic force microscope [34–38]. Thus, it is highly likely that the heightened cellular activity on the NG surface is dictated by the interplay of physical and chemical attributes as well as the mechanisms that govern the interaction between cells and nanometre scale surface. It is postulated that the nanoscale features in the NG surface trigger alterations in cell adhesion (cell binding) ability, surface activity (electron work function, charge carrier density), grain boundary state and surface energetics. This is because of an increase in grain boundary density in the NG surface compared to the CG counterpart. This significantly impacts the functionality of cells at the bio-nano interface (cell–substrate interface) and is the focus of the proposed research. A fundamental understanding of the physical and chemical mechanisms involved in modulating the cellular activities on the NG surface is vital for the development of nanotechnologies.

Thus, the ongoing studies on physical and chemical attributes of NG and CG surfaces in a single material will uncover the molecular mechanisms that are involved in the nano-bio interface interactions. Furthermore, regardless of the current understating of how nanoscale features affect the cellular functionality of osteoblasts (as depicted in Figures 2–7), it is crucial to address two fundamental questions from a transformative point of view. Doing so will contribute to the sustainable development of nanotechnology. These questions include an inquiry into the contrasting influence of nanoscale structure on the unique physical and chemical attributes of the NG surface compared to that of the CG counterpart, and how such contrasting influence impacted the functionality of cells at the bio-nano interface (i.e. cell–substrate interactions). Uncovering the mechanism responsible for connecting the nanoscale feature of the NG surface and how it affects its grain boundary state, surface energetics and surface activity such as electron work function and charge carrier would be a major contribution to the field. In addition, addressing the question of how such effects would impact biological functions such as cell adhesion, proliferation, protein synthesis, and cell signalling would be vital to our mechanistic understanding of the interaction of nanostructured surfaces with cells in the context of biological functions.

The discovery of physical and chemical mechanisms that are responsible for modulating cellular functions could potentially contribute to the fundamental understanding of the science concerning bio-nano interactions. Furthermore, it will enable us to decipher the pathways and mechanisms for nanostructure-induced favourable cellular functions by integrating biological functions with chemical and physical attributes. A deep understanding of cell–substrate interactions can eventually aid in the development of engineered surfaces that possess specific physical and chemical attributes, and this could potentially result in a desired biological

response. The scientific principles underlying bio-nano interactions can be readily extrapolated to other biomedical devices such as metallic systems such as titanium and cobalt-based alloys and non-metallic systems such as ceramics and polymer nanocomposites, owing to their similar structure–property relationships. This is pertinent to the process of osseointegration and the replacement of hard tissues.

Disclosure statement

No potential conflict of interest was reported by the author(s).

Funding

The work was supported by the National Science Foundation. R.D.K. Misra and Aladin M. Boriek are grateful to the National Science Foundation for financial support through grant # CBET 2224942 (Program Manager: Dr Nora F. Savage).

References

[1] Borsari V, Giavaresi G, Fini M, et al. Physical characterization of different-roughness titanium surfaces, with and without hydroxyapatite coating, and their effect on human osteoblast-like cells. J Biomed Mater Res, Part B. 2005;75B:359–368.
[2] Balasundaram G, Webster T. Increased osteoblast adhesion on nano-grained titanium modified with KRSR. J Biomed Mater Res Part A. 2007;80:602–611.
[3] Willman G. Coating of implants with hydroxyapatite-material connections between bone and metal. Adv Eng Mater. 1999;1:95–105.
[4] Kay S, Thapa A, Haberstroh KM, et al. Nanostructured polymer/nanophase ceramic composites enhance osteoblast and chondrocyte adhesion. Tissue Eng. 2002;8:573-561. DOI:10.1089/10763270260424114
[5] McManus AJ, Doremus RH, Siegel RW, et al. Evaluation of cytocompatibility and bending modulus of nanoceramic/polymer composites. J Biomed Mater Res A. 2005;72:98–106.
[6] Webster TJ, Ergun C, Doremus RH, et al. Enhanced function of osteoblast on nanophase ceramics. Biomaterials. 2000;67:1803–1810.
[7] Webster TJ, Siegel RW, Bizios R. Osteoblast adhesion on nanophase ceramics. Biomaterials. 1999;20:1221–1227.
[8] Thapa A, Webster TJ, Haberstroth KM. Polymers with nano-dimensional surface features enhance smooth muscle cell adhesion. J Biomed Mater Res A. 2003;67:1374–1383.
[9] Webster TJ, Smith TA. Increased osteoblast function on PLGA composites containing nanophase titania. J Biomed Mater Res A. 2005;74A:677–686.
[10] Faghihi S, Azari F, Zhilyeav AP, et al. Nanostructuring of a titanium material by high-pressure torsion improves pre-osteoblast attachment. Adv Mater Res. 2007;19:1069–1073.
[11] Faghihi S, Azari F, Zhilyeav AP, et al. Cellular and molecular interactions between MC3T3-E1 pre-osteoblasts and nanostructured titanium produced by high-pressure torsion. Biomaterials. 2007;28:3887–3895.
[12] Song R, Ponge D, Raabe D, et al. Microstructure and crystallographic texture of an ultrafine-grained C-Mn steel and their evolution during warm deformation and annealing. Acta Materialia. 2005;53:845–858.
[13] Humphreys FJ, Prangnell PB, Bowen JR, et al. Developing stable fine-grain microstructures by large strain deformation. Philos Trans R Soc Of London A. 1999;357:1663–1681.
[14] Pitan C, Hashimoto T, Kawazoe M, et al. Microstructure and texture evolution in ECAE processed A5056. Mater Sci Eng A. 2000;280:62–68.
[15] Zhu YT, Lowe TC, Langdon TG. Performance and applications of nanostructured materials produced by severe plastic deformation. Scripta Materialia. 2004;51:825–830.
[16] Park KT, Kim YS, Shin DH. Microstructural stability of ultrafine-grained low-carbon steel containing vanadium fabricated by intense plastic straining. Metall Mater Trans A. 2001;32A:2373–2381.
[17] Tsuji N, Saito Y, Utsunomiya H, et al. Ultra-fine grained bulk steel produced by accumulative roll-bonding (ARB) process. Scripta Materialia. 1999;40:795–800.
[18] Saito Y, Utsunomiya H, Tsuji N, et al. Novel ultra-high straining process for bulk materials-development of the accumulative roll-bonding (ARB) process. Acta Materialia. 1999;47:579–583.
[19] Costa ALM, Reis ACC, Kestens L, et al. Ultra grain refinement and hardening of IF-steel during accumulative roll-bonding. Mat Sci Eng A. 2005;406:279–285.
[20] Zhilyaev AP, Nurislamova GV, Kim BK, et al. Experimental parameters influencing grain refinement and microstructural evolution during high-pressure torsion. Acta Materialia. 2003;51:753–765.
[21] Ivanisenko Y, Lojkowski W, Valiev RZ, et al. The mechanism of formation of nanostructure and dissolution of cementite in a pearlitic steel during high-pressure torsion. Acta Materialia. 2003;51:5555–5570.
[22] Beladi H, Kelly GL, Shokouhi A, et al. Effect of thermomechanical parameters on the critical strain for ultrafine ferrite formation through hot torsion testing. Mat Sci Eng A. 2004;367:152–161.
[23] Sauvage X, Wetscher F, Pareige P. Mechanical alloying of Cu and Fe induced by severe plastic deformation of a Cu-Fe composite. Acta Materialia. 2005;53:2127–2135.
[24] Belyakov A, Sakai T, Miura H, et al. Substructures and internal stresses developed under warm severe deformation of austenitic stainless steel. Scripta Materialia. 2000;42:319–325.
[25] Lianxi H, Yuping L, Erde W, et al. Ultrafine grained structure and mechanical properties of an LY12 Al alloy prepared by repetitive upsetting-extrusion. Mat Sci Eng A. 2006;422:327–332.
[26] Ning H, Li X, Meng L, et al. Effect of Ni and Mo on microstructure and mechanical properties of grey cast iron. Mater Technol. 2023;38:2172991.
[27] Guo L, Su X, Dai L, et al. Strain ageing embrittlement behaviour of X80 self-shielded flux-cored girth weld metal. Mater Technol. 2023;38:2164978.
[28] Yang C, Xu H, Wang Y, et al. Hot Tearing analysis and process optimisation of the fire face of Al-Cu

alloy cylinder head based on MAGMA numerical simulation. Mater Technol. 2023;38:2165245.
[29] Li Q, Zuo H, Feng J, et al. Strain rate and temperature sensitivity on the flow behaviour of a duplex stainless steel during hot deformation. Mater Technol. 2023;38:2166216.
[30] Misra RDK, Injeti YSY, Somani MC. The significance of deformation mechanisms on the fracture behavior of phase-reversion induced nanostructured austenitic stainless steel. Sci Rep Nat. 2018;8:7908. 1-13.
[31] Misra RDK, Challa VSA, Venkatsurya PKC, et al. Interplay between grain structure, deformation mechanisms, and austenite stability in phase reversion-induced nanograined/ultrafine-grained ferrous alloy. Acta Materialia. 2015;84:339–348.
[32] Misra RDK, Nayak S, Mali S, et al. On the significance of nature of strain-induced martensite on phase-reversion induced nano grained/ultrafine--grained (NG/UFG) austenitic stainless steel. Metall Mater Trans A. 2015;41A:3–12.
[33] Misra RDK. Materials Letters. 2023.
[34] Misra RDK, Thein-Han WW, Pesacreta TC, et al. Favorable modulation of pre-osteoblasts response to nanograined/ultrafine-grained structures in austenitic stainless steel. Adv Mater. 2009;21:1280–1285.
[35] Misra RDK, Thein-Han WW, Pesacreta TC, et al. Cellular response of pre-osteoblasts to nanograined/ultrafine-grained structures. Acta Biomaterialia. 2009;5:1455–1467.
[36] Misra RDK, Thein-Han WW, Pesacreta TC, et al. Cellular biological significance of nanograined/ultrafine-grained structures: interaction with fibroblasts. Acta Biomaterialia. 2010;6:3339–3348.
[37] Misra RDK, Thein-Han WW, Mali SA, et al. Cellular activity of bioactive nanograined/ultrafine-grained materials. Acta Biomaterialia. 2010;6:2826–2835.
[38] Venkatsurya PKC, Thein-Han WW, Misra RDK, et al. Advancing nanograined/ultrafine-grained structures for metal implant: interplay between grooving of nano/ultrafine grains and cellular R.
[39] Lowe TC, Reiss RA, Illescas, PE et al. Effect of surface grain boundary density on preosteoblast proliferation on titanium. Mater Res Lett. 2020;8:239.
[40] Le Saux G, Magneau A, Gunanrathan K. Spacing of integrin ligands influences signal transduction in endothelial cells. Biophysics J. 2011;101:764–773.